# On the relation between seismic interferometry and the migration resolution function

Jan Thorbecke[1] and Kees Wapenaar[1]

## ABSTRACT

Seismic interferometry refers to the process of retrieving new seismic responses by crosscorrelating seismic observations at different receiver locations. Seismic migration is the process of forming an image of the subsurface by wavefield extrapolation. Comparing the expressions for backward propagation known from migration literature with the Green's function representations for seismic interferometry reveals that these seemingly distinct concepts are mathematically equivalent. The frequency-domain representation for the resolution function of migration is identical to that for the Green's function retrieved by seismic interferometry (or its square, in the case of double focusing). In practice, they differ because the involved Green's functions in seismic interferometry are all defined in the actual medium, whereas in migration one of the Green's functions is defined in a background medium.

## INTRODUCTION

Seismic interferometry is a relatively new branch of geophysics that constructs new seismic responses by crosscorrelating traces recorded at different receiver locations. Applications exist for seismic exploration data with controlled sources (Schuster, 2001; Schuster et al., 2004; Bakulin and Calvert, 2004, 2006; Wapenaar, 2006) as well as for passive seismic data from natural sources (Rickett and Claerbout, 1999; Wapenaar et al., 2002; Campillo and Paul, 2003; Draganov et al., 2007). For an overview, we refer to the supplement of the 2006 July-August issue of GEOPHYSICS, which also contains contributions from authors of other disciplines.

One particular approach of deriving expressions for seismic interferometry is based on the reciprocity theory (Wapenaar, 2004; Weaver and Lobkis, 2004; van Manen et al., 2005). This approach leads to exact integral representations of impulse responses (Green's functions) in terms of crosscorrelations. These representations closely resemble those in seismic migration and Born inversion (Wapenaar et al., 2005; van Manen et al., 2005; Korneev and Bakulin, 2006).

We start this paper by briefly reviewing the Green's function representation for seismic interferometry and then discuss the remarkable similarity with the representation of the basic resolution function for migration. In both cases, the resulting representation is that of a so-called homogeneous Green's function. We continue by showing that the same homogeneous Green's function representation appears in Born inversion and migration by double focusing. The representations we use in this paper have been published and can all be derived from Rayleigh's reciprocity theorem. In this paper, we highlight how the same mathematical expressions occur in different areas, discuss their difference of use, and show their aesthetic similarities.

## REPRESENTATION OF THE GREEN'S FUNCTION FOR INTERFEROMETRY

Consider a Green's function $G(\mathbf{x}, \mathbf{x}_A, t)$ for an inhomogeneous, lossless acoustic medium where $\mathbf{x}$ and $\mathbf{x}_A$ are the Cartesian coordinate vectors for the observation and source points, respectively, and where $t$ denotes time. We define the temporal Fourier transform as $\hat{G}(\mathbf{x}, \mathbf{x}_A, \omega) = \int_{-\infty}^{\infty} \exp(-j\omega t) G(\mathbf{x}, \mathbf{x}_A, t) dt$, where $j$ is the imaginary unit and $\omega$ the angular frequency. Assuming the unit point source at $\mathbf{x}_A$ is of the volume injection rate type, the wave equation for $\hat{G}(\mathbf{x}, \mathbf{x}_A, \omega)$ reads

$$\rho \partial_i (\rho^{-1} \partial_i \hat{G}(\mathbf{x}, \mathbf{x}_A, \omega)) + \frac{\omega^2}{c^2} \hat{G}(\mathbf{x}, \mathbf{x}_A, \omega)$$

$$= -j\omega\rho\delta(\mathbf{x} - \mathbf{x}_A). \tag{1}$$

Here, $c = c(\mathbf{x})$ and $\rho = \rho(\mathbf{x})$ are the propagation velocity and mass density of the inhomogeneous medium and $\partial_i$ denotes the partial derivative in the $x_i$-direction (Einstein's summation convention applies to repeated subscripts). The representation of $\hat{G}$, as derived for seis-

mic interferometry from Rayleigh's reciprocity theorem (Rayleigh, 1878), reads

$$\hat{G}_h(\mathbf{x}_A,\mathbf{x}_B,\omega) = \oint_{\partial\mathbb{D}} \frac{-1}{j\omega\rho(\mathbf{x})}\Big(\hat{G}^*(\mathbf{x}_A,\mathbf{x},\omega)\partial_i\hat{G}(\mathbf{x}_B,\mathbf{x},\omega)$$

$$- (\partial_i\hat{G}^*(\mathbf{x}_A,\mathbf{x},\omega))\hat{G}(\mathbf{x}_B,\mathbf{x},\omega)\Big)n_i\mathrm{d}^2\mathbf{x}, \quad (2)$$

with

$$\hat{G}_h(\mathbf{x}_A,\mathbf{x}_B,\omega) \equiv \hat{G}(\mathbf{x}_A,\mathbf{x}_B,\omega) + \hat{G}^*(\mathbf{x}_A,\mathbf{x}_B,\omega), \quad (3)$$

where $\partial\mathbb{D}$ is an arbitrary closed surface with outward-pointing normal vector $\mathbf{n} = (n_1,n_2,n_3)$ and the asterisk denotes complex conjugation (Wapenaar et al., 2005). The points $\mathbf{x}_A$ and $\mathbf{x}_B$ are both situated inside $\partial\mathbb{D}$; the medium may be inhomogeneous inside as well as outside $\partial\mathbb{D}$. The term $\hat{G}_h(\mathbf{x}_A,\mathbf{x}_B,\omega)$ is called the homogeneous Green's function (after Oristaglio, 1989) because it obeys wave equation 1 without the source term.

Note that if we skip the $j\omega$ factor in the source term on the right-hand side of equation 1, we obtain a representation similar to equation 2, with a minus sign in the right-hand side of equation 3 (van Manen et al., 2005).

For the interpretation of the seismic interferometric representation (equation 2), we refer to Figure 1. The Green's functions under the integral are responses of monopole and dipole sources at $\mathbf{x}$ on the boundary $\partial\mathbb{D}$, observed by receivers at $\mathbf{x}_A$ and $\mathbf{x}_B$. The products $\hat{G}^*\partial_i\hat{G}$ and $(\partial_i\hat{G}^*)\hat{G}$ correspond to crosscorrelations at these observation points; the integral is taken along the sources on $\partial\mathbb{D}$. The Green's function $\hat{G}_h(\mathbf{x}_A,\mathbf{x}_B,\omega)$ in the left-hand side is the Fourier transform of $G(\mathbf{x}_A,\mathbf{x}_B,t) + G(\mathbf{x}_A,\mathbf{x}_B,-t)$, which is the superposition of the response at $\mathbf{x}_A$ resulting from an impulsive source at $\mathbf{x}_B$ and its time-reversed version. The Green's function $G(\mathbf{x}_A,\mathbf{x}_B,t)$ is causal, so it can be obtained by taking the causal part of this superposition.

Equation 2 is the basis for seismic interferometry. It shows how the crosscorrelation of observations at two receiver positions yields the response at one of the receiver positions as if there were a source at the other. Under far-field conditions, assuming that outside $\partial\mathbb{D}$ the medium is homogeneous (i.e., assuming unidirectional waves at $\partial\mathbb{D}$), we may approximate $n_i\partial_i\hat{G}$ by $-jk\hat{G}$, with $k = \omega/c$. With this approximation, equation 2 simplifies to
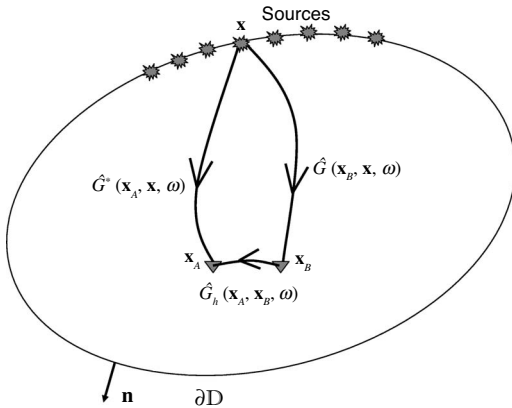


Figure 1. Green's function representation for seismic interferometry (equation 2). The "rays" in this figure represent the full responses between the source and receiver points, including primary and multiple scattering as a result of inhomogeneities inside as well as outside $\partial\mathbb{D}$.

$$\hat{G}_h(\mathbf{x}_A,\mathbf{x}_B,\omega) \approx \frac{2}{\rho c}\oint_{\partial\mathbb{D}} \hat{G}^*(\mathbf{x}_A,\mathbf{x},\omega)\hat{G}(\mathbf{x}_B,\mathbf{x},\omega)\mathrm{d}^2\mathbf{x}, \quad (4)$$

or, in the time domain,

$$G(\mathbf{x}_A,\mathbf{x}_B,t) + G(\mathbf{x}_A,\mathbf{x}_B,-t)$$

$$\approx \frac{2}{\rho c}\oint_{\partial\mathbb{D}} G(\mathbf{x}_A,\mathbf{x},-t) * G(\mathbf{x}_B,\mathbf{x},t)\mathrm{d}^2\mathbf{x}, \quad (5)$$

where the asterisk denotes convolution.

We conclude this section by considering the situation of uncorrelated noise sources $N(\mathbf{x},t)$ on $\partial\mathbb{D}$, with $\langle N(\mathbf{x},-t)*N(\mathbf{x}',t)\rangle = \delta(\mathbf{x} - \mathbf{x}')S(t)$, where $\langle\cdot\rangle$ denotes a spatial ensemble average and $S(t)$ the autocorrelation of the noise. For the observed wavefields at $\mathbf{x}_A$ and $\mathbf{x}_B$, we may write $p^{\mathrm{obs}}(\mathbf{x}_A,t) = \oint_{\partial\mathbb{D}}G(\mathbf{x}_A,\mathbf{x},t)*N(\mathbf{x},t)\mathrm{d}^2\mathbf{x}$ and $p^{\mathrm{obs}}(\mathbf{x}_B,t) = \oint_{\partial\mathbb{D}}G(\mathbf{x}_B,\mathbf{x}',t)*N(\mathbf{x}',t)\mathrm{d}^2\mathbf{x}'$, respectively. Evaluating the crosscorrelation of these wavefields yields

$$\langle p^{\mathrm{obs}}(\mathbf{x}_A,-t) * p^{\mathrm{obs}}(\mathbf{x}_B,t)\rangle$$

$$= \oint_{\partial\mathbb{D}} G(\mathbf{x}_A,\mathbf{x},-t) * G(\mathbf{x}_B,\mathbf{x},t) * S(t)\mathrm{d}^2\mathbf{x}. \quad (6)$$

Combining this with equation 5, we obtain

$$\{G(\mathbf{x}_A,\mathbf{x}_B,t) + G(\mathbf{x}_A,\mathbf{x}_B,-t)\} * S(t)$$

$$\approx \frac{2}{\rho c}\langle p^{\mathrm{obs}}(\mathbf{x}_A,-t) * p^{\mathrm{obs}}(\mathbf{x}_B,t)\rangle. \quad (7)$$

This expression shows that the Green's function between $\mathbf{x}_A$ and $\mathbf{x}_B$ is obtained from the direct crosscorrelation of observed fields at $\mathbf{x}_A$ and $\mathbf{x}_B$, resulting from a distribution of noise sources at $\partial\mathbb{D}$. In most practical situations, sources are not available on a closed surface. Modifications for one-sided illumination, either by controlled sources at the surface or natural noise sources in the subsurface, are discussed by Wapenaar (2006).

## REPRESENTATION OF THE BASIC RESOLUTION FUNCTION FOR MIGRATION

As mentioned in the introduction, the Green's function representation for seismic interferometry (equation 2) closely resembles that in seismic migration and inversion. Using source-receiver reciprocity, we interchange $\mathbf{x}$ and $\mathbf{x}_B$ in the Green's functions on the right-hand side of equation 2, which gives

$$\hat{G}_h(\mathbf{x}_A,\mathbf{x}_B,\omega) = \oint_{\partial\mathbb{D}} \frac{-1}{j\omega\rho(\mathbf{x})}\Big(\hat{G}^*(\mathbf{x}_A,\mathbf{x},\omega)\partial_i\hat{G}(\mathbf{x},\mathbf{x}_B,\omega)$$

$$- (\partial_i\hat{G}^*(\mathbf{x}_A,\mathbf{x},\omega))\hat{G}(\mathbf{x},\mathbf{x}_B,\omega)\Big)n_i\mathrm{d}^2\mathbf{x}. \quad (8)$$

Despite this minor change, the interpretation is completely different (see Figure 2). The Green's functions $\hat{G}(\mathbf{x},\mathbf{x}_B,\omega)$ and $(-1/j\omega\rho(\mathbf{x}))\partial_i\hat{G}(\mathbf{x},\mathbf{x}_B,\omega)$ represent the data in terms of the acoustic pressure and particle velocity observed at receiver point $\mathbf{x}$ on the surface $\partial\mathbb{D}$ from a source at $\mathbf{x}_B$ in the subsurface. (For an actual seismic experiment with sources at the surface, the "source" at $\mathbf{x}_B$ is a secondary source, representing a diffractor; a more complete data model is discussed in the next section.) The Green's functions $\hat{G}^*(\mathbf{x}_A,\mathbf{x},\omega)$ and $(1/j\omega\rho(\mathbf{x}))\partial_i\hat{G}^*(\mathbf{x}_A,\mathbf{x},\omega)$ back-propagate these data

from the surface to any point $\mathbf{x}_A$ in the subsurface. Porter (1970) uses this relation for holographic imaging of monochromatic waves in a homogeneous medium.

Hence, the wavefield originating from $\mathbf{x}_B$ is recorded at the surface $\partial\mathbb{D}$, and one can interpret the recorded field as Huygens' sources, emitting back-propagating waves to any point $\mathbf{x}_A$ inside $\partial\mathbb{D}$ and forming a monochromatic image. The resulting field, with all contributions of all Huygens' sources on the surface $\partial\mathbb{D}$, consists of converging and subsequently diverging wavefields around the source position $\mathbf{x}_B$. This monochromatic image represents the resolution function of the configuration because it shows how a source at $\mathbf{x}_B$ is reconstructed from measurements at $\partial\mathbb{D}$. For a perfectly converging field, one would expect intuitively that the left-hand side of equation 8 represents a spatial delta pulse at the source position $\mathbf{x}_B$. However, according to equation 8, the resolution function is represented by the homogeneous Green's function $\hat{G}_h(\mathbf{x}_A,\mathbf{x}_B,\omega)$. For a homogeneous medium, it is given by

$$\hat{G}_h(\mathbf{x}_A,\mathbf{x}_B,\omega) = j\omega\rho\left(\frac{\mathrm{e}^{-jkr}}{4\pi r} - \frac{\mathrm{e}^{jkr}}{4\pi r}\right) = \omega\rho\frac{\sin(kr)}{2\pi r}, \quad (9)$$

with $k = \omega/c$ and $r = |\mathbf{x}_A - \mathbf{x}_B|$. This function has its maximum for $r \to 0$, where the amplitude is equal to $\omega^2\rho/2\pi c$. The width of the main lobe (measured at the zero crossings) is equal to the wavelength $\lambda = 2\pi/k$. When the wavelength approaches zero ($\lambda \to 0$), the focusing becomes perfect and equation 9 approaches a delta function.

Equation 8 can be seen as the basic resolution function for migration. To obtain the resolution of the migration of a broadband point source at $\mathbf{x}_B$, we need to multiply both sides of equation 8 by the spectrum $\hat{s}(\omega)$ of the source at $\mathbf{x}_B$, apply an inverse Fourier transform to the left-hand side, and evaluate the result for $t = 0$ (which is the imaging condition in migration). For a homogeneous medium, we obtain for the inverse Fourier transform of the left-hand side (using equation 9):

$$\hat{G}_h(\mathbf{x}_A,\mathbf{x}_B,\omega)\hat{s}(\omega) \Rightarrow \frac{\rho}{4\pi r}\{\dot{s}(t - r/c) - \dot{s}(t + r/c)\}, \quad (10)$$

where $\dot{s}(t)$ denotes the time derivative of the source wavelet. Evaluated at $t = 0$, this gives $(\rho/4\pi r)\{\dot{s}(-r/c) - \dot{s}(r/c)\}$, which is the broadband migration resolution function.

Of course, the analysis presented here is valid only when the wavefield is measured on a closed surface. In practice, the acquisition is always limited to a finite part of an open surface, which means that the actual resolution function is a spatially bandlimited version of the resolution function discussed here. This issue is addressed by Berkhout (1984), Miller et al. (1987), Schuster and Hu (2000), Gelius et al. (2002), and many others; a more detailed analysis is not needed to understand the relations discussed in this paper.

Our aim was to review the insight of Porter (1970) and others that the resolution function of an imaging system is given by the Green's function of the medium plus its time-reversed version [the latter is a result of the fact that there is not a sink at the image position to absorb the converging wavefield; see Derode et al. (2003) and van Manen et al. (2005)]. The resemblance between the Green's function representation for interferometry and the resolution function is striking. In hindsight, the basic theory for seismic interferometry was available in the 1970s. An important difference is that in the interferometric relations 2 and 4, the Green's functions on the right-hand side represent measured wavefields, whereas in equation 8, $\hat{G}(\mathbf{x},\mathbf{x}_B,\omega)$ is the

measured wavefield but the back propagator $\hat{G}^*(\mathbf{x}_A,\mathbf{x},\omega)$ is based on a background model. Hence, whereas $\hat{G}_h(\mathbf{x}_A,\mathbf{x}_B,\omega)$ in equations 2 and 4 represents the Green's function in the actual medium (including all multiple scattering), the determination of $\hat{G}_h(\mathbf{x}_A,\mathbf{x}_B,\omega)$ in equation 8 is in practice limited by the accuracy of the background model. This observation is also made by Korneev and Bakulin (2006).

In the following sections, we review work of Oristaglio (1989) on Born inversion and of Berkhout (1997), Thorbecke (1997), and Schuster and Hu (2000) on migration by double focusing and show their relations with the homogeneous Green's function representation.

## RESOLUTION FUNCTION FOR BORN INVERSION AND DOUBLE FOCUSING

The Born approximation of a scattered wavefield for a compressibility contrast $\Delta\kappa(\mathbf{x})$ in a domain $\mathbb{D}$ with background parameters $\rho(\mathbf{x})$ and $\kappa(\mathbf{x})$ (with $\kappa^{-1} = \rho c^2$) can be expressed as (Oristaglio, 1989)

$$\hat{p}^s(\mathbf{x}_r,\mathbf{x}_s,\omega) = -j\omega\int_{\mathbb{D}}\hat{G}(\mathbf{x}_r,\mathbf{x}',\omega)\Delta\kappa(\mathbf{x}')\hat{G}(\mathbf{x}',\mathbf{x}_s,\omega)\mathrm{d}^3\mathbf{x}'.$$

(11)

Analogous to equation 8, we define back propagation of the scattered field $\hat{p}^s(\mathbf{x}_r,\mathbf{x}_s,\omega)$ from the receiver locations $\mathbf{x}_r$ to any $\mathbf{x}$ in the scattering medium again by a Kirchhoff-Helmholtz integral according to

$$\hat{\Phi}(\mathbf{x},\mathbf{x}_s,\omega) = \oint_{\partial\mathbb{D}}\frac{-1}{j\omega\rho(\mathbf{x}_r)}\big(\hat{G}^*(\mathbf{x},\mathbf{x}_r,\omega)\partial_i^r\hat{p}^s(\mathbf{x}_r,\mathbf{x}_s,\omega)$$

$$- (\partial_i^r\hat{G}^*(\mathbf{x},\mathbf{x}_r,\omega))\hat{p}^s(\mathbf{x}_r,\mathbf{x}_s,\omega)\big)n_i\mathrm{d}^2\mathbf{x}_r, \quad (12)$$

where $\hat{G}^*(\mathbf{x},\mathbf{x}_r,\omega)$ is a model-based back-propagating Green's function and $\partial_i^r$ denotes differentiation with respect to the receiver coordinate $\mathbf{x}_r$. Physically, $\hat{\Phi}(\mathbf{x},\mathbf{x}_s,\omega)$ can be interpreted as an approximation of the scattered field $\hat{p}^s(\mathbf{x},\mathbf{x}_s,\omega)$ in $\mathbb{D}$, except that $\hat{\Phi}(\mathbf{x},\mathbf{x}_s,\omega)$ also
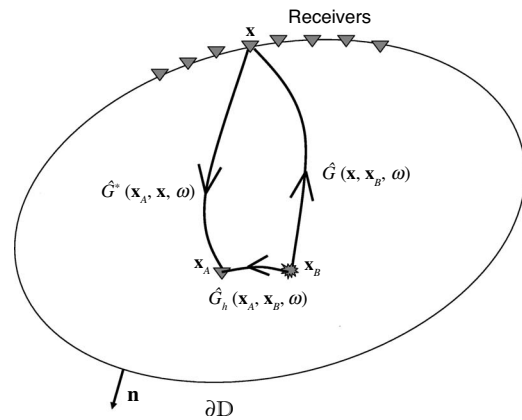


Figure 2. Representation of the basic resolution function (equation 8). The forward model of the data is represented by the ray from the source at $\mathbf{x}_B$ to the receiver at $\mathbf{x}$. Back propagation is represented by the ray from $\mathbf{x}$ to the image point $\mathbf{x}_A$. The resolution function is represented by the ray from the source at $\mathbf{x}_B$ to the image point $\mathbf{x}_A$.

contains a noncausal part because in equation 12 there is no sink absorbing the converging wavefield. Related to the common focal point (CFP) work of Berkhout (1997) and Thorbecke (1997), equation 12 corresponds to focusing the receiver array to a point in $\mathbb{D}$ for any available source position $\mathbf{x}_s$. Back-propagating the receiver array is a common process in most seismic migration techniques (Claerbout, 1971).

Substituting the Born approximation of the scattered field of equation 11 into the expression for backward propagation (equation 12) and interchanging the order of integration yields

$$\hat{\Phi}(\mathbf{x},\mathbf{x}_s,\omega) = \int_{\mathbb{D}} \oint_{\partial\mathbb{D}} \frac{1}{\rho(\mathbf{x}_r)} \Big( \hat{G}^*(\mathbf{x},\mathbf{x}_r,\omega)(\partial_i^r \hat{G}(\mathbf{x}_r,\mathbf{x}',\omega))$$
$$- (\partial_i^r \hat{G}^*(\mathbf{x},\mathbf{x}_r,\omega))\hat{G}(\mathbf{x}_r,\mathbf{x}',\omega)\Big)$$
$$\times \Delta\kappa(\mathbf{x}')\hat{G}(\mathbf{x}',\mathbf{x}_s,\omega)n_i \mathrm{d}^2\mathbf{x}_r \mathrm{d}^3\mathbf{x}' \qquad (13)$$

or

$$\hat{\Phi}(\mathbf{x},\mathbf{x}_s,\omega) = -j\omega \int_{\mathbb{D}} \hat{G}_h(\mathbf{x},\mathbf{x}',\omega)\Delta\kappa(\mathbf{x}')\hat{G}(\mathbf{x}',\mathbf{x}_s,\omega)\mathrm{d}^3\mathbf{x}', \qquad (14)$$

where it is important to observe that the representation for the homogeneous Green's function $\hat{G}_h(\mathbf{x},\mathbf{x}',\omega)$ is the same as in equation 8, but with $\mathbf{x}_A$ and $\mathbf{x}_B$ replaced by $\mathbf{x}$ and $\mathbf{x}'$, respectively, and the integration carried out over the receiver locations $\mathbf{x}_r$. According to equation 14, this homogeneous Green's function propagates the contribution of the secondary source $\Delta\kappa(\mathbf{x}')\hat{G}(\mathbf{x}',\mathbf{x}_s,\omega)$ from $\mathbf{x}'$ to $\mathbf{x}$ and results in a causal and a noncausal contribution.

The field at $\mathbf{x}$ is the result of back propagating the waves measured at the surface $\partial\mathbb{D}$. With multiple sources, there is a field $\hat{\Phi}(\mathbf{x},\mathbf{x}_s,\omega)$ for each source position $\mathbf{x}_s$. This additional degree of freedom can be used to apply back propagation of the source array using the model-based Green's function $\hat{G}^*(\mathbf{x}'',\mathbf{x}_s,\omega)$. Similarly, the back-propagated wavefield of the source array is defined as
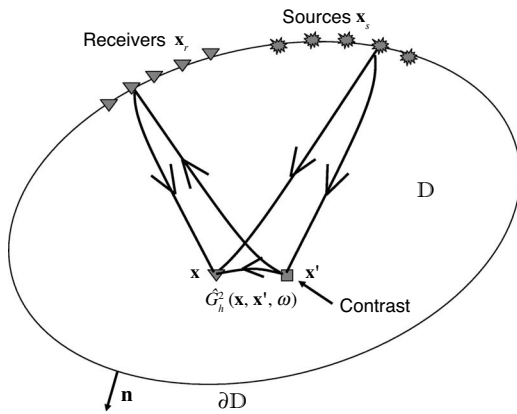


Figure 3. Representation of the resolution function in Born inversion and confocal imaging. The forward model of the data is represented by the ray from the source at $\mathbf{x}_s$, via the diffractor at $\mathbf{x}'$, to the receiver at $\mathbf{x}_r$. Double focusing is represented by the rays from $\mathbf{x}_s$ and $\mathbf{x}_r$ to the confocal image point $\mathbf{x}$. The resolution function is represented by the ray from the diffractor at $\mathbf{x}'$ to the image point $\mathbf{x}$.

$$\hat{\Phi}(\mathbf{x},\mathbf{x}'',\omega) = \oint_{\partial\mathbb{D}} \frac{-1}{j\omega\rho(\mathbf{x}_s)} \Big( \hat{G}^*(\mathbf{x}'',\mathbf{x}_s,\omega)\partial_i^s \hat{\Phi}(\mathbf{x},\mathbf{x}_s,\omega)$$
$$- (\partial_i^s \hat{G}^*(\mathbf{x}'',\mathbf{x}_s,\omega))\hat{\Phi}(\mathbf{x},\mathbf{x}_s,\omega)\Big)n_i \mathrm{d}^2\mathbf{x}_s, \qquad (15)$$

where $\partial_i^s$ denotes differentiation with respect to the source coordinate $\mathbf{x}_s$. Physically, $\hat{\Phi}(\mathbf{x},\mathbf{x}'',\omega)$ can be interpreted as an approximation of the scattered field $\hat{p}^s(\mathbf{x},\mathbf{x}'',\omega)$ for a virtual source focused at $\mathbf{x}''$ in $\mathbb{D}$, except that $\hat{\Phi}(\mathbf{x},\mathbf{x}'',\omega)$ contains an additional noncausal contribution because in equation 15 there is again no sink to absorb the converging wavefield. Substituting the back-propagated field representation of equation 14 into the back-propagating integral for the sources (equation 15), interchanging the order of integration, and using source-receiver reciprocity of the Green's functions gives the double-focusing result

$$\hat{\Phi}(\mathbf{x},\mathbf{x}'',\omega) = \int_{\mathbb{D}} \oint_{\partial\mathbb{D}} \frac{1}{\rho(\mathbf{x}_s)} \hat{G}_h(\mathbf{x},\mathbf{x}',\omega)\Delta\kappa(\mathbf{x}')$$
$$\times \Big( \hat{G}^*(\mathbf{x}'',\mathbf{x}_s,\omega)(\partial_i^s \hat{G}(\mathbf{x}_s,\mathbf{x}',\omega))$$
$$- (\partial_i^s \hat{G}^*(\mathbf{x}'',\mathbf{x}_s,\omega))\hat{G}(\mathbf{x}_s,\mathbf{x}',\omega)\Big)n_i \mathrm{d}^2\mathbf{x}_s \mathrm{d}^3\mathbf{x}' \qquad (16)$$

or

$$\hat{\Phi}(\mathbf{x},\mathbf{x}'',\omega) = -j\omega \int_{\mathbb{D}} \hat{G}_h(\mathbf{x},\mathbf{x}',\omega)\Delta\kappa(\mathbf{x}')$$
$$\times \hat{G}_h(\mathbf{x}',\mathbf{x}'',\omega)\mathrm{d}^3\mathbf{x}', \qquad (17)$$

with $\hat{G}_h(\mathbf{x}',\mathbf{x}'',\omega) = \hat{G}_h(\mathbf{x}'',\mathbf{x}',\omega)$ the same as in equation 8 but this time with the integration carried out over the source locations $\mathbf{x}_s$. An expression similar to equation 17 can be derived in a similar way for a density contrast.

When $\mathbf{x} \neq \mathbf{x}''$, then $\hat{\Phi}(\mathbf{x},\mathbf{x}'',\omega)$ represents a bifocal image (Berkhout, 1997). For $\mathbf{x} = \mathbf{x}''$, it becomes a confocal image (see Figure 3). Using the symmetry of $\hat{G}_h(\mathbf{x}',\mathbf{x}'',\omega)$ and setting $\mathbf{x} = \mathbf{x}''$, equation 17 can be written as

$$\hat{\Phi}(\mathbf{x},\mathbf{x},\omega) = -j\omega \int_{\mathbb{D}} \hat{G}_h^2(\mathbf{x},\mathbf{x}',\omega)\Delta\kappa(\mathbf{x}')\mathrm{d}^3\mathbf{x}', \qquad (18)$$

where the repeated $\mathbf{x}$ in $\hat{\Phi}(\mathbf{x},\mathbf{x},\omega)$ denotes that the receiver array and the source array have been back-propagated to the same point. The term $\hat{G}_h^2(\mathbf{x},\mathbf{x}',\omega)$ is the resolution function for Born inversion and confocal imaging because it shows how material property contrast $\Delta\kappa(\mathbf{x}')$ for all $\mathbf{x}'$ in $\mathbb{D}$ contributes to the image obtained at point $\mathbf{x}$.

We conclude this section by showing how property contrast $\Delta\kappa(\mathbf{x})$ is related to the double-focusing result $\hat{\Phi}(\mathbf{x},\mathbf{x},\omega)$, following Oristaglio (1989). For $\mathbf{x}$ in the neighborhood of $\mathbf{x}'$, it is reasonable to assume locally homogeneous background medium parameters. Using equation 9, we obtain

$$\frac{\partial}{\partial\omega}\left( \frac{\hat{G}_h^2(\mathbf{x},\mathbf{x}',\omega)}{\omega^2} \right) \approx \frac{\rho(\mathbf{x})\hat{G}_h(\mathbf{x},\mathbf{x}',2\omega)}{4\pi\omega c(\mathbf{x})}. \qquad (19)$$

An important property of $\hat{G}_h(\mathbf{x},\mathbf{x}',\omega)$ is that its inverse Fourier transform evaluated at $t = 0$ (which is equivalent to integration over all frequencies) yields the spatial delta function $\kappa^{-1}(\mathbf{x}')\delta(\mathbf{x} - \mathbf{x}')$ (see

Appendix A in Oristaglio, 1989). Combining this property with equations 18 and 19, we obtain

$$\frac{1}{2\pi}\int_{-\infty}^{\infty}\frac{4\pi\omega c(\mathbf{x})}{\rho(\mathbf{x})}\frac{\partial}{\partial\omega}\left(\frac{\hat{\Phi}(\mathbf{x},\mathbf{x},\omega)}{-j\omega^3}\right)\mathrm{d}(2\omega)$$

$$=\frac{1}{2\pi}\int_{\mathbb{D}}\mathrm{d}^3\mathbf{x}'\Delta\kappa(\mathbf{x}')\int_{-\infty}^{\infty}\hat{G}_h(\mathbf{x},\mathbf{x}',2\omega)\mathrm{d}(2\omega)$$

$$=\frac{\Delta\kappa(\mathbf{x})}{\kappa(\mathbf{x})}, \qquad (20)$$

where $\hat{\Phi}(\mathbf{x},\mathbf{x},\omega)$ is the double-focusing result of equation 18. Equation 20 shows how this double-focusing result can be used to obtain quantitative information about the contrast function $\Delta\kappa(\mathbf{x})$.

## RESOLUTION FUNCTION FOR STANDARD PRESTACK MIGRATION

The analysis of the resolution function in the previous section was done under the assumption that back propagation takes place with Kirchhoff-Helmholtz-type integrals, in which back propagating Green's functions as well as their derivatives are applied to wavefields and their derivatives (see equations 12 and 15 for the back propagation of receivers and sources, respectively). In seismic migration, each of these two-term integrals is usually approximated by a one-term integral containing a (derivative of a) Green's function acting on the wavefield. Here, we show that, with some approximations, the resolution function for standard prestack migration can again be written as the square of the homogeneous Green's function.

As the starting point for our analysis, we consider a result of Schuster and Hu (2000), who derive resolution functions for seismic migration using the Born approximation and the adjoint of the forward modeling operator. Their final expression for the migrated image (with our definition of the Green's function) is

$$m_{\mathrm{mig}}(\mathbf{x})=\int_{\mathrm{model\ space}}\hat{\Gamma}(\mathbf{x},\mathbf{x}',\omega)m(\mathbf{x}')\mathrm{d}^3\mathbf{x}', \qquad (21)$$

where

$$\hat{\Gamma}(\mathbf{x},\mathbf{x}',\omega)=\left(\frac{4\pi}{j\omega\rho}\right)^4\int\int_{\mathrm{data\ space}}\hat{G}^*(\mathbf{x}_r,\mathbf{x},\omega)\hat{G}^*(\mathbf{x},\mathbf{x}_s,\omega)$$

$$\times\hat{G}(\mathbf{x}_r,\mathbf{x}',\omega)\hat{G}(\mathbf{x}',\mathbf{x}_s,\omega)\mathrm{d}^2\mathbf{x}_r\mathrm{d}^2\mathbf{x}_s. \qquad (22)$$

(Actually, they considered an integral along the receiver coordinate $\mathbf{x}_r$ only, but for our analysis we include the integral along the source coordinate $\mathbf{x}_s$). Schuster and Hu (2000) loosely named $\hat{\Gamma}(\mathbf{x},\mathbf{x}',\omega)$ the migration Green's function. We show that $\hat{\Gamma}(\mathbf{x},\mathbf{x}',\omega)$ is indeed (the square of) a Green's function.

Reorganizing the terms under the integral and assuming again that the sources and receivers occupy a closed surface $\partial\mathbb{D}$, we obtain

$$\hat{\Gamma}(\mathbf{x},\mathbf{x}',\omega)=\left(\frac{4\pi}{j\omega\rho}\right)^4\oint_{\partial\mathbb{D}}\oint_{\partial\mathbb{D}}\hat{G}^*(\mathbf{x},\mathbf{x}_r,\omega)\hat{G}(\mathbf{x}',\mathbf{x}_r,\omega)$$

$$\times\hat{G}^*(\mathbf{x},\mathbf{x}_s,\omega)\hat{G}(\mathbf{x}',\mathbf{x}_s,\omega)\mathrm{d}^2\mathbf{x}_r\mathrm{d}^2\mathbf{x}_s. \qquad (23)$$

Comparing the right-hand side with the far-field approximation of the homogeneous Green's function representation (equation 4), we obtain

$$\hat{\Gamma}(\mathbf{x},\mathbf{x}',\omega)\approx\frac{64\pi^4 c^2}{\omega^4\rho^2}\hat{G}_h^2(\mathbf{x},\mathbf{x}',\omega). \qquad (24)$$

Schuster and Hu (2000) show that a finite acquisition surface results in a filtered version of the migration Green's function $\hat{\Gamma}(\mathbf{x},\mathbf{x}',\omega)$ which, according to our derivation, is proportional to the square of the homogeneous Green's function $\hat{G}_h(\mathbf{x},\mathbf{x}',\omega)$.

## CONCLUSIONS

We have shown that the representations for seismic interferometry and for migration resolution functions are equivalent mathematically and yield, in both cases, the homogeneous Green's function $\hat{G}_h(\mathbf{x},\mathbf{x}',\omega)$ or its square, in the case of double focusing. In seismic interferometry, $\hat{G}_h(\mathbf{x},\mathbf{x}',\omega)$ is obtained from measurements and therefore represents the Green's function in the actual medium (including multiple scattering), whereas the accuracy of the migration Green's function is limited by the accuracy of the background model. Throughout this article, the analysis was based on the assumption of a closed acquisition surface. In practice, the acquisition is always restricted to a finite part of an open surface. The effect of a finite acquisition surface on the migration resolution function has been analyzed by various authors. Based on the observed relation between interferometry and the resolution function, a similar analysis could be applied to the results of seismic interferometry for the situation of a finite-source distribution. Of course, this analysis should be done with care because of the differences mentioned above.

## ACKNOWLEDGMENTS

## REFERENCES

Bakulin, A., and R. Calvert, 2004, Virtual source: New method for imaging and 4D below complex overburden: 74th Annual International Meeting, SEG, Expanded Abstracts, 2477–2480.
——, 2006, The virtual source method: Theory and case study: Geophysics, **71**, no. 4, SI139–SI150.
Berkhout, A. J., 1984, Seismic resolution: A quantitative analysis of resolving power of acoustical echo techniques: Geophysical Press.
——, 1997, Pushing the limits of seismic imaging, part I: Prestack migration in terms of double dynamic focusing: Geophysics, **62**, 937–953.
Campillo, M., and A. Paul, 2003, Long-range correlations in the diffuse seismic coda: Science, **299**, 547–549.
Claerbout, J. F., 1971, Toward a unified theory of reflector mapping: Geophysics, **36**, 467–481.
Derode, A., E. Larose, M. Tanter, J. de Rosny, A. Tourin, M. Campillo, and M. Fink, 2003, Recovering the Green's function from field-field correlations in an open scattering medium (L): Journal of the Acoustical Society of America, **113**, 2973–2976.
Draganov, D., K. Wapenaar, W. Mulder, J. Singer, and A. Verdel, 2007, Retrieval of reflections from seismic background-noise measurements: Geo-

physical Research Letters, **34**, L04305-1–L04305-4.

Gelius, L.-J., I. Lecomte, and H. Tabti, 2002, Analysis of the resolution function in seismic prestack depth imaging: Geophysical Prospecting, **50**, 505–515.

Korneev, V., and A. Bakulin, 2006, On the fundamentals of the virtual source method: Geophysics, **71**, no. 3, A13–A17.

Miller, D., M. Oristaglio, and G. Beylkin, 1987, A new slant on seismic imaging: Migration and integral geometry: Geophysics, **52**, 943–964.

Oristaglio, M. L., 1989, An inverse scattering formula that uses all the data: Inverse Problems, **5**, 1097–1105.

Porter, R. P., 1970, Diffraction-limited, scalar image formation with holograms of arbitrary shape: Journal of the Optical Society of America, **60**, 1051–1059.

Rayleigh, J. W. S., 1878, The theory of sound, vol. II: Dover Publications, Inc. (reprint 1945).

Rickett, J., and J. Claerbout, 1999, Acoustic daylight imaging via spectral factorization: Helioseismology and reservoir monitoring: The Leading Edge, **18**, 957–960.

Schuster, G. T., 2001, Theory of daylight/interferometric imaging: Tutorial: 63rd Annual Conference and Exhibition, EAGE, Extended Abstracts, A32-1–A32-4.

Schuster, G. T., and J. Hu, 2000, Green's function for migration: Continuous recording geometry: Geophysics, **65**, 167–175.

Schuster, G. T., J. Yu, J. Sheng, and J. Rickett, 2004, Interferometric/daylight seismic imaging: Geophysical Journal International, **157**, 838–852.

Thorbecke, J. W., 1997, Common focus point technology: Ph.D. dissertation, Delft University of Technology.

van Manen, D.-J., J. O. A. Robertsson, and A. Curtis, 2005, Modeling of wave propagation in inhomogeneous media: Physical Review Letters, **94**, 164301-1–164301-4.

Wapenaar, K., 2004, Retrieving the elastodynamic Green's function of an arbitrary inhomogeneous medium by cross correlation: Physical Review Letters, **93**, 254301-1–254301-4.

———, 2006, Green's function retrieval by cross-correlation in case of one-sided illumination: Geophysical Research Letters, **33**, L19304-1–L19304-6.

Wapenaar, K., D. Draganov, J. Thorbecke, and J. Fokkema, 2002, Theory of acoustic daylight imaging revisited: 72nd Annual International Meeting, SEG, Expanded Abstracts, 2269–2272.

Wapenaar, K., J. Fokkema, and R. Snieder, 2005, Retrieving the Green's function in an open system by cross-correlation: A comparison of approaches (L): Journal of the Acoustical Society of America, **118**, 2783–2786.

Weaver, R. L., and O. I. Lobkis, 2004, Diffuse fields in open systems and the emergence of the Green's function (L): Journal of the Acoustical Society of America, **116**, 2731–2734.